European Journal of Medicinal Chemistry 46 (2011) 4311–4323

Contents lists available at ScienceDirect

European Journal of Medicinal Chemistry

journal homepage: http://www.elsevier.com/locate/ejmech

Original article

Imidazo[2,1-*b*]thiazole guanylhydrazones as RSK2 inhibitors [1]

Aldo Andreani [a,*], Massimiliano Granaiola [a], Alberto Leoni [a], Alessandra Locatelli [a], Rita Morigi [a], Mirella Rambaldi [a], Lucilla Varoli [a], Deborah Lannigan [b], Jeff Smith [c], Dominic Scudiero [d], Sudhir Kondapaka [e], Robert H. Shoemaker [e,**]

[a] *Dipartimento di Scienze Farmaceutiche, Università di Bologna, Via Belmeloro 6, 40126 Bologna, Italy*
[b] *Center for Cell Signaling, Department of Microbiology, University of Virginia, Charlottesville, VA 22908, USA*
[c] *Center for Cell Signaling, Department of Pathology, University of Virginia, Charlottesville, VA 22908, USA*
[d] *SAIC-Frederick, National Cancer Institute at Frederick, Frederick, MD 21702, USA*
[e] *Screening Technologies Branch, Developmental Therapeutics Program, Division of Cancer Treatment and Diagnosis, National Cancer Institute at Frederick, Frederick, MD 21702, USA*

ARTICLE INFO

Article history:
Received 4 May 2011
Received in revised form
24 June 2011
Accepted 1 July 2011
Available online 8 July 2011

Keywords:
Imidazo[2,1-*b*]thiazole
Guanylhydrazones
Antitumor activity
RSK2

ABSTRACT

The activity of a series of imidazo[2,1-*b*]thiazole guanylhydrazones as inhibitors of p90 ribosomal S6 kinase 2 (RSK2) is described. It was found that a small subset of compounds show both potent inhibition of RSK2 kinase activity and tumor cell growth in vitro. Detailed study of one of the most active compounds indicates a high degree of selectivity for inhibition of RSK2 compared to a spectrum of other related kinases. Selective inhibition of the MCF-7 breast tumor cell line compared to MCF-10A non-transformed cells, as well as selective inhibition of the biomarker GSK3 provides evidence that the compounds can affect the RSK2 target in cells.

1. Introduction

We have recently reported synthesis and initial biological characterization of a series of imidazo[2,1-*b*]thiazole guanylhydrazones as potential anticancer derivatives [2]. These compounds displayed a broad range of potency as in vitro growth inhibitors and the patterns of activity generated in the NCI-60 screen were suggestive of multiple mechanisms of action.

For further studies on the antitumor activity and mechanism(s) of action, a new series has been synthesized taking into account the features which, in the previous papers, gave good results such as the 2-chloroimidazothiazole system, the 2,5-dichlorothienyl and 2,5-dimethoxy-4-nitrophenyl groups at the 6 position of the imidazothiazole system, the substitution of the imidazothiazole with analogous systems (imidazothiadiazole, imidazobenzothiazole and imidazopyridine) and the substitution of the usual guanylhydrazone chain with analogous chains. In this new series we wish to consider the following situations (see Schemes 1 and 2).

A) Substituents at the 6 position of the imidazothiazole or at the corresponding position of analogous systems:
   - 2,5-dichlorothiophene on imidazothiazole and analogous systems: **17a**, **18a**, **30a** and **34a**.
   - 2,5-dimethoxy-4-nitrophenyl group on imidazothiazole-like systems (on the imidazothiazole system it had been considered in previous papers) [2,3]: **18b**, **30b** and **34b**.
B) Replacement of the guanylhydrazone chain with a chain containing an imidazoline ring. This has been done on selected systems: **24a**, **25c**, **31a** and **35a**.
C) Fluoro derivatives were synthesized following the example of many drugs whose activity has been enhanced by incorporation of fluorine [4]: **17e,j**, **20e–l** and **21e,j**.
D) Comparison with previously published analogs: **17d,n**, **19d**, **20m**, **22o** and **23o**.

Abbreviations: RSK2, p90 ribosomal S6 kinase 2; GSK3, glycogen synthase kinase 3; NCI, National Cancer Institute; DTP, Developmental Therapeutics Program; DMSO, dimethylsulphoxide; GI, growth inhibition; TGI, total growth inhibition; LC, lethal concentration; BEC, Biological Evaluation Committee; TPA, 12-O-tetradecanoylphorbol-13-acetate; IMAP, Immobilized Metal ion Affinity-based fluorescence Polarization; PVDF, Polyvinylidene Fluoride; HRP, horseradish peroxidase.

* Corresponding author. Tel.: +39 51 2099714; fax: +39 51 2099734.
** Corresponding author. Tel.: +301 846 6845.
E-mail addresses: aldo.andreani@unibo.it (A. Andreani), shoemakr@mail.nih.gov (R.H. Shoemaker).

0223-5234/$ – see front matter © 2011 Elsevier Masson SAS. All rights reserved.
doi:10.1016/j.ejmech.2011.07.001

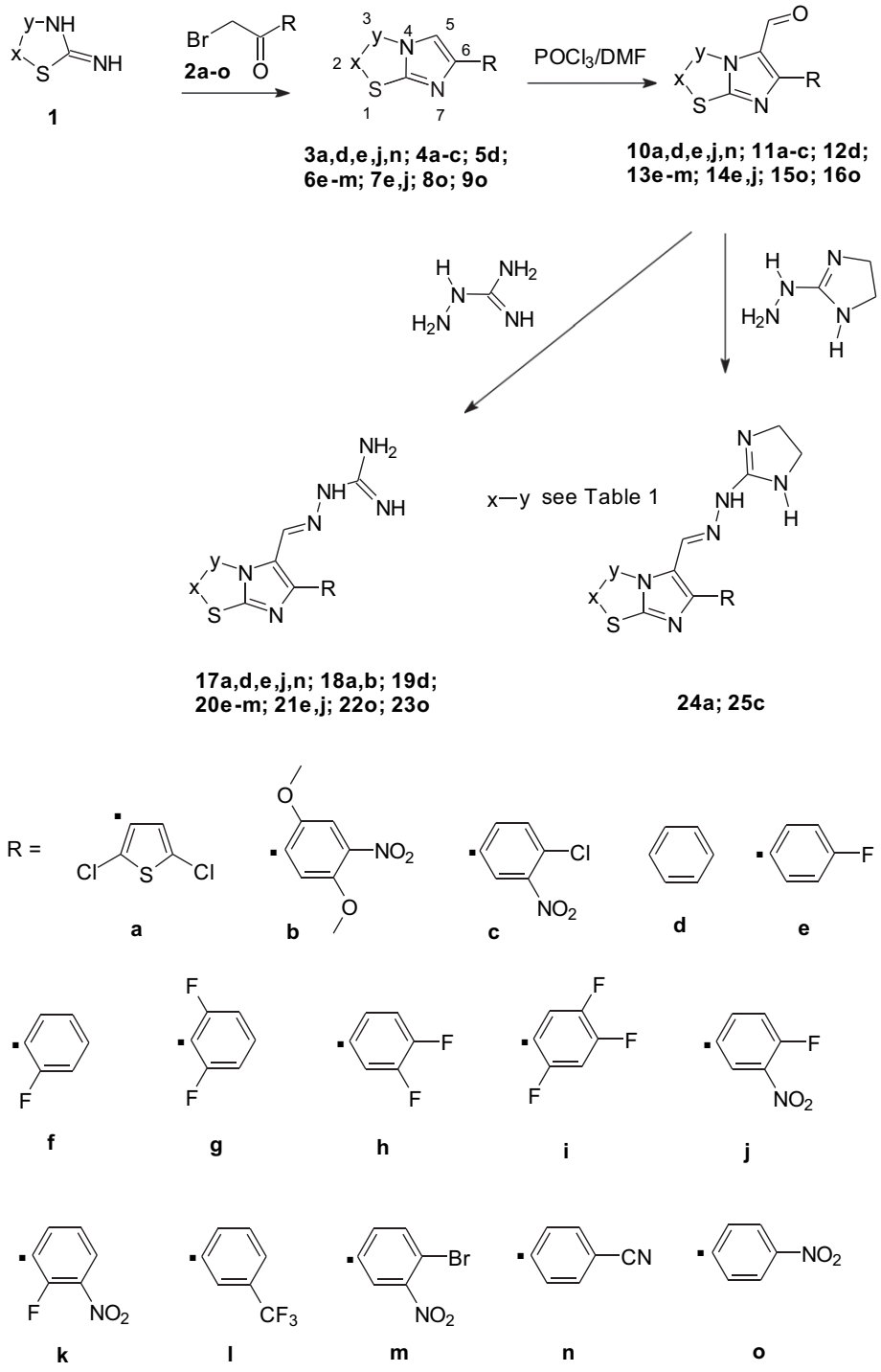

Scheme 1.

Molecular-targeted screening of the NCI chemical repository has recently led to identification of a bis-guanylhydrazone as a lead chemotype for inhibition of CHK2 kinase [5]. Based on the structural similarity of this compound to the imidazo[2,1-*b*]thiazole guanylhydrazones, we evaluated this class of compounds (those described here and others selected from previous papers) as kinase inhibitors. While no potent inhibitors of CHK2 were found, several potent and highly selective inhibitors of RSK2 were identified.

RSK2 has been identified as a potential oncology drug development target based on its role in MAP kinase signaling [6] and more recently on its importance for the RAS-ERK pathway as it effects tumor cell invasion [7]. Since only a limited number of small molecule inhibitors have been previously reported [8,9], we were interested to pursue this series in detail.

2. Chemistry

The hydrazones **17a**,**d**,**e**,**j**,**n**, **18a**,**b**, **19d**, **20e**–**m**, **21e**,**j**, **22o**, **23o**, **24a** and **25c** (Scheme 1, Table 1), **30a**,**b**, **31a**, **34a**,**b** and **35a** (Scheme

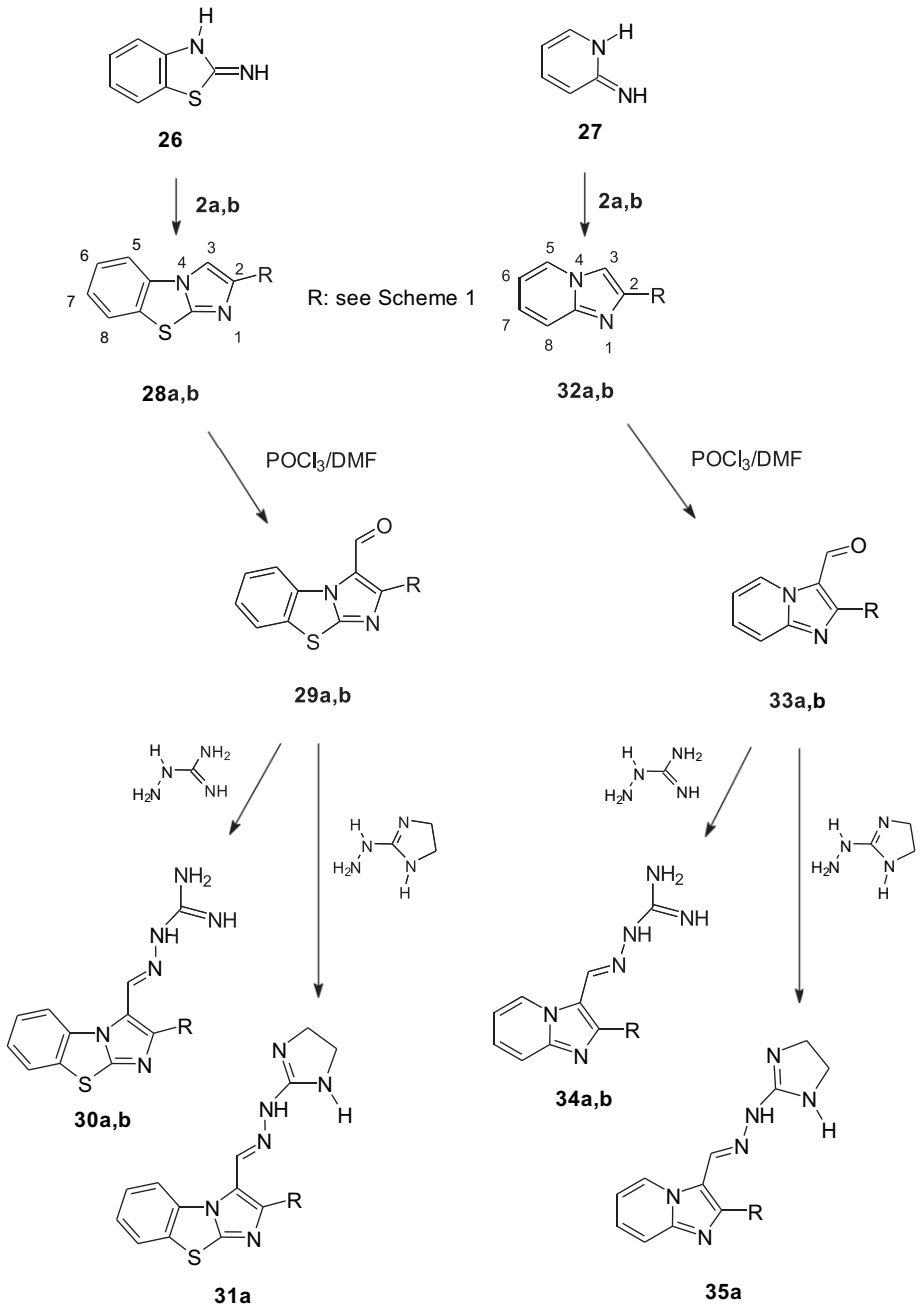

Scheme 2.

2, Table 2) were prepared by reaction between an aldehyde and aminoguanidine or 2-hydrazino-2-imidazoline.

The new starting aldehydes **10a**,**e**,**j**,**n**, **11a**,**b**, **12d**, **13e**–**k**,**m**, **14e**,**j**, **15o**, **16o**, **29a**,**b** and **33a**,**b** were obtained by means of the Vilsmeier reaction on the new compounds **3a**,**e**,**j**,**n**, **4a**,**b**, **6f**–**k**,**m**, 7**e**,**j**, **8o**, **9o**, **28a**,**b**, **32a**,**b** prepared in turn from the appropriate 2-amino-derivative (**1**, **26**, **27**) and the bromoketones **2a**–**o**.

The other starting materials were prepared according to the literature: **5d** [10], **6e** [11], **10d** [12], **11c** [2], and **13l** [13]. The starting bromoacetophenones **2a**–**i** and **2l**–**o** are commercially available, whereas the synthesis of **2j**,**k** is reported under the Experimental section. The IR and ^{1}H NMR spectra of the new compounds are in agreement with the assigned structures (see Experimental section).

3. Biology

3.1. Antitumor activity

In a preliminary test, compounds were tested at a single high concentration (10^{-5} M) in the full NCI 60 cell panel (NCI 60 Cell One-Dose Screen). This panel is organized into subpanels representing leukemia, melanoma and cancers of lung, colon, kidney, ovary, breast, prostate and central nervous system. Only compounds which satisfy pre-determined threshold inhibition criteria in a minimum number of cell lines will progress to the full 5-concentration assay. The threshold inhibition criteria for progression to the 5-concentration screen was selected to efficiently capture compounds with anti-proliferative activity based on

Table 1
New compounds described in Scheme 1.

Comp.[a]	x–y	Formula	MW	Mp, °C
3a	ClC=CH	$C_9H_3Cl_3N_2S_2$	309.63	156–158
3e	ClC=CH	$C_{11}H_6ClFN_2S$	252.70	190–193
3j	ClC=CH	$C_{11}H_5ClFN_3O_2S$	297.70	185–187
3n	ClC=CH	$C_{12}H_6ClN_3S$	259.72	240–243
4a	H_3CC=N	$C_9H_5Cl_2N_3S_2$	290.20	111–113
4b	H_3CC=N	$C_{13}H_{12}N_4O_4S$	320.33	204–206
6f	HC=CH	$C_{11}H_7FN_2S$	218.25	120–122
6g	HC=CH	$C_{11}H_6F_2N_2S$	236.24	80–82
6h	HC=CH	$C_{11}H_6F_2N_2S$	236.24	150–151
6i	HC=CH	$C_{11}H_5F_3N_2S$	254.23	160–162
6j	HC=CH	$C_{11}H_6FN_3O_2S$	263.25	225–230
6k	HC=CH	$C_{11}H_6FN_3O_2S$	263.25	230–233
6m	HC=CH	$C_{11}H_6BrN_3O_2S$	324.16	212–215
7e	H_3CC=CH	$C_{12}H_9FN_2S$	232.28	200–201
7j	H_3CC=CH	$C_{12}H_8FN_3O_2S$	277.28	160–162
8o	FC=CH	$C_{11}H_6FN_3O_2S$	263.25	255–257
9o	BrC=CH	$C_{11}H_6BrN_3O_2S$	324.16	245–247
10a	ClC=CH	$C_{10}H_3Cl_3N_2OS_2$	337.64	192–194
10e	ClC=CH	$C_{12}H_6ClFN_2OS$	280.71	173–175
10j	ClC=CH	$C_{12}H_5ClFN_3O_3S$	325.71	183–185
10n	ClC=CH	$C_{13}H_6ClN_3OS$	287.73	248–250
11a	H_3CC=N	$C_{10}H_5Cl_2N_3OS_2$	318.21	150–152
11b	H_3CC=N	$C_{14}H_{12}N_4O_5S$	348.34	242–244
12d	H_2NC=N	$C_{11}H_8N_4OS$	244.28	>335
13e	HC=CH	$C_{12}H_7FN_2OS$	246.26	170–172
13f	HC=CH	$C_{12}H_7FN_2OS$	246.26	152–155
13g	HC=CH	$C_{12}H_6F_2N_2OS$	264.25	110–112
13h	HC=CH	$C_{12}H_6F_2N_2OS$	264.25	198–200
13i	HC=CH	$C_{12}H_5F_3N_2OS$	282.24	260–263
13j	HC=CH	$C_{12}H_6FN_3O_3S$	291.26	245–250
13k	HC=CH	$C_{12}H_6FN_3O_3S$	291.26	235–238
13m	HC=CH	$C_{12}H_6BrN_3O_3S$	352.17	253–255
14e	H_3CC=CH	$C_{13}H_9FN_2OS$	260.29	160–162
14j	H_3CC=CH	$C_{13}H_8FN_3O_3S$	305.29	221–223
15o	FC=CH	$C_{12}H_6FN_3O_3S$	291.26	225–228
16o	BrC=CH	$C_{12}H_6BrN_3O_3S$	352.17	276–278
17a	ClC=CH	$C_{11}H_7Cl_3N_6S_2 \cdot HCl$	430.17	296–298
17d	ClC=CH	$C_{13}H_{11}ClN_6S \cdot HCl$	355.25	278–280 dec.
17e	ClC=CH	$C_{13}H_{10}ClFN_6S \cdot HCl$	374.25	330–332 dec.
17j	ClC=CH	$C_{13}H_9ClFN_7O_2S \cdot HCl$	418.24	>335
17n	ClC=CH	$C_{14}H_{10}ClN_7 \cdot HCl$	380.26	>335
18a	H_3CC=N	$C_{11}H_9Cl_2N_7S_2 \cdot HCl$	410.74	290–292
18b	H_3CC=N	$C_{15}H_{16}N_8O_4S \cdot HCl$	440.87	279–281
19d	H_2NC=N	$C_{12}H_{12}N_8S \cdot HCl$	336.81	259–260
20e	HC=CH	$C_{13}H_{11}FN_6S \cdot HCl$	338.79	265–270
20f	HC=CH	$C_{13}H_{11}FN_6S \cdot HCl$	338.79	245–250 dec.
20g	HC=CH	$C_{13}H_{10}F_2N_6S \cdot HCl$	356.78	315–317
20h	HC=CH	$C_{13}H_{10}F_2N_6S \cdot HCl$	356.78	267–270 dec.
20i	HC=CH	$C_{13}H_9F_3N_6S \cdot HCl$	374.77	325–328
20j	HC=CH	$C_{13}H_{10}FN_7O_2S \cdot HCl$	383.79	315–320 dec.
20k	HC=CH	$C_{13}H_{10}FN_7O_2S \cdot HCl$	383.79	288–290
20l	HC=CH	$C_{14}H_{11}F_3N_6S \cdot HCl$	388.80	257–260 dec.
20m	HC=CH	$C_{13}H_{10}BrN_7O_2S \cdot HCl$	444.70	294–296 dec.
21e	H_3CC=CH	$C_{14}H_{13}FN_6S \cdot HCl$	352.82	330–332 dec.
21j	H_3CC=CH	$C_{14}H_{12}FN_7O_2S \cdot HCl$	397.82	220–225 dec.
22o	FC=CH	$C_{13}H_{10}FN_7O_2S \cdot HCl$	383.79	>335
23o	BrC=CH	$C_{13}H_{10}BrN_7O_2S \cdot HCl$	444.70	>335
24a	ClC=CH	$C_{13}H_9Cl_3N_6S_2 \cdot HBr$	500.66	288–290
25c	H_3CC=N	$C_{15}H_{13}ClN_8O_2S \cdot HBr$	485.75	280–282

[a] According to Scheme 1, the letter is related to the substituent at the 6 position (R).

careful analysis of historical DTP screening data. The result is expressed as the percent growth of treated cells (unpublished results).

Five compounds (**18b**, **19d**, **20f**,**g** and **34b**) were not considered active enough to enter the 5-concentration test.

The others were subjected to the subsequent screen. They were dissolved in dimethylsulphoxide (DMSO) and evaluated using five concentrations at ten-fold dilutions, the highest being 10^{-4} M

Table 2
New compounds described in Scheme 2.

Comp.	Formula	MW	Mp, °C
28a	$C_{13}H_6Cl_2N_2S_2$	325.24	187–189
28b	$C_{17}H_{13}N_3O_4S$	355.37	268–270
29a	$C_{14}H_6Cl_2N_2OS_2$	353.25	194–196
29b	$C_{18}H_{13}N_3O_5S$	383.38	263–265
30a	$C_{15}H_{10}Cl_2N_6S_2 \cdot HCl$	445.78	281–283
30b	$C_{19}H_{17}N_7O_4S \cdot HCl$	475.91	267–269
31a	$C_{17}H_{12}Cl_2N_6S_2HBr$	516.27	275–277
32a	$C_{11}H_6Cl_2N_2S$	269.15	150–153
32b	$C_{15}H_{13}N_3O_4$	299.28	188–190
33a	$C_{12}H_6Cl_2N_2OS$	297.16	169–171
33b	$C_{16}H_{13}N_3O_5$	327.29	248–250
34a	$C_{13}H_{10}Cl_2N_6S \cdot HCl$	389.69	295–297
34b	$C_{17}H_{17}N_7O_4 \cdot HCl$	419.82	286–288
35a	$C_{15}H_{12}Cl_2N_6S \cdot HBr$	460.18	296–298

following 48 h incubation. Table 3 reports the results obtained (Methyl-GAG is reported for comparison purposes), expressed as the negative log of the molar concentration at three assay endpoints: the 50% growth inhibitory power (pGI_{50}), the cytostatic effect (pTGI = Total Growth Inhibition) and the cytotoxic effect (pLC_{50}). They showed a mean pGI_{50} range between 6.51 and 4.20. The mean GI_{50} values expressed as micromolar concentrations are reported in Table 4.

For 13 compounds the 5-concentration test was repeated and no significant differences were found. For these compounds the data reported in Table 3 are the mean values between the two experiments. Compounds **17a**,**d**,**n**, **20m**, **22o**, **23o** and **30a**, were submitted to BEC (Biological Evaluation Committee) for a possible future development.

In light of the NCI-60 results, the following considerations may be made:

- The introduction of a 2,5-dimethoxy-4-nitrophenyl group at the 6 position of the imidazothiazole system led to potent cytotoxic compounds [3] but this didn't happen in the analogous systems. Among the three compounds prepared (**18b**, **30b** and **34b**), only **30b** entered the 5-concentration screen and showed mean pGI_{50} 5.75. The difference between the average concentration that caused 50% growth inhibition and the concentration that killed 50% of the cells was about 1 log unit, therefore toxicity is lower than for most of the other compounds.
  The substituent 2,5-dichlorothiophene was more interesting, leading to very active compounds when it was introduced in the imidazobenzothiazole (**30a**, mean pGI_{50} 6.34) and in the 2-chloroimidazothiazole (**17a**, mean pGI_{50} 6.03). These two compounds were selected by BEC for possible additional studies.
- Replacement of the guanylhydrazone chain with a chain containing an imidazoline ring lead to decrease in activity which was significant for compound **31a** (mean pGI_{50} 4.20 vs. 6.34 of the corresponding guanylhydrazone) and weak for compound **25c** (mean pGI_{50} 5.71 vs. 5.90 of the corresponding guanylhydrazone) [2].
- Among the 6-fluorophenyl-imidazothiazoles, only **20f** and **20g** were inactive in the preliminary test whereas all the others were tested on the 5-concentration screen with a mean pGI_{50} ranging from 5.61 to 5.89. It is interesting to point out that, within this range, the activity was higher in compounds bearing both fluorine and nitro group (see for example **17j**, **20j**, **20k** and **21j**).

Table 3
Nine subpanels at five concentrations: growth inhibition, cytostatic and cytotoxic activity of the selected compounds: see Supplementary data (Figure S1) for the complete list of cell lines employed.

Comp[a]	Modes	Leukemia	NSCLC	Colon	CNS	Melanoma	Ovarian	Renal	Prostate	Breast	MG-MID[b]
17a[c]	pGI_{50}	6.68	5.80	6.41	5.90	5.88	5.83	5.84	5.89	6.17	6.03
	pTGI	6.09	5.46	5.87	5.56	5.58	5.50	5.52	5.54	5.85	5.65
	pLC_{50}	5.34	5.08	5.37	5.23	5.18	5.09	5.21	5.29	5.25	5.19
17d[c]	pGI_{50}	5.70	5.08	5.61	5.07	5.47	5.04	5.05	5.16	5.35	5.28
	pTGI	5.27	4.68	5.20	4.70	5.10	4.67	4.65	4.70	4.96	4.89
	pLC_{50}	4.73	4.32	4.76	4.33	4.74	4.32	4.30	4.33	4.52	4.49
17e[c]	pGI_{50}	6.37	5.75	5.95	5.78	5.77	5.75	5.76	5.79	5.89	5.85
	pTGI	5.65	5.45	5.58	5.50	5.49	5.47	5.50	5.52	5.54	5.51
	pLC_{50}	–	5.09	5.25	5.23	5.22	5.07	5.24	5.26	5.20	5.16
17j[c]	pGI_{50}	6.52	5.72	6.03	5.80	5.75	5.72	5.75	5.88	5.93	5.87
	pTGI	5.88	5.39	5.64	5.49	5.45	5.40	5.45	5.54	5.45	5.48
	pLC_{50}	4.22	4.91	5.22	5.10	5.13	5.04	5.17	5.25	4.97	5.03
17n[c]	pGI_{50}	6.51	5.78	6.37	5.89	5.81	5.79	5.75	6.07	6.03	5.97
	pTGI	5.73	5.40	5.92	5.56	5.43	5.37	5.41	5.64	5.55	5.53
	pLC_{50}	–	4.95	5.42	5.06	4.90	4.94	5.05	5.24	4.87	5.02
18a	pGI_{50}	5.44	5.55	5.72	5.72	5.73	5.68	5.64	5.53	5.60	5.63
	pTGI	4.51	5.10	5.38	5.37	5.43	5.34	5.25	5.08	5.20	5.20
	pLC_{50}	4.02	4.31	4.87	4.99	4.98	4.72	4.78	4.71	4.49	4.63
20e[c]	pGI_{50}	5.70	5.45	5.64	5.78	5.61	5.52	5.61	5.62	5.64	5.61
	pTGI	5.26	5.02	5.30	5.37	5.28	5.13	5.23	5.18	5.31	5.23
	pLC_{50}	4.88	4.57	4.94	4.99	4.92	4.60	4.91	4.70	4.90	4.83
20h	pGI_{50}	5.79	5.71	5.77	5.80	5.76	5.78	5.75	5.74	5.69	5.75
	pTGI	5.42	5.34	5.50	5.51	5.49	5.49	5.47	5.39	5.37	5.44
	pLC_{50}	5.06	4.96	5.22	5.23	5.22	5.20	5.19	5.03	5.06	5.13
20i	pGI_{50}	5.74	5.71	5.74	5.77	5.73	5.73	5.67	5.59	5.65	5.71
	pTGI	5.36	5.35	5.44	5.48	5.46	5.43	5.33	5.12	5.33	5.39
	pLC_{50}	4.79	4.91	5.11	5.21	5.19	5.09	4.97	4.67	4.91	5.00
20j	pGI_{50}	5.83	5.64	5.70	5.74	5.64	5.65	5.65	5.76	5.75	5.68
	pTGI	–	5.25	5.30	5.45	5.32	5.31	5.32	5.50	5.26	5.29
	pLC_{50}	–	4.67	4.81	5.20	4.82	4.43	4.72	5.24	4.73	4.75
20k	pGI_{50}	5.81	5.76	5.68	5.81	5.71	5.76	5.56	5.78	5.56	5.70
	pTGI	5.45	5.43	5.30	5.51	5.40	5.48	5.13	5.50	5.27	5.37
	pLC_{50}	4.78	4.86	5.02	5.22	5.01	5.20	4.74	5.23	4.71	4.96
20l	pGI_{50}	5.86	5.60	5.73	5.73	5.74	5.60	5.68	5.63	5.67	5.69
	pTGI	5.44	5.14	5.43	5.35	5.47	5.21	5.31	5.15	5.34	5.33
	pLC_{50}	5.00	4.73	5.11	4.91	5.20	4.81	4.85	4.59	4.98	4.94
20m[c]	pGI_{50}	6.37	5.77	6.32	5.91	5.79	5.77	5.72	5.80	5.90	5.92
	pTGI	5.92	5.44	5.86	5.59	5.50	5.39	5.35	5.53	5.55	5.55
	pLC_{50}	5.45	4.99	5.33	5.31	5.16	5.08	5.00	5.25	5.18	5.17
21e[c]	pGI_{50}	5.90	5.77	5.80	5.79	5.77	5.75	5.78	5.78	5.76	5.78
	pTGI	5.50	5.46	5.51	5.50	5.49	5.45	5.50	5.52	5.40	5.47
	pLC_{50}	5.25	5.14	5.23	5.17	5.23	5.04	5.22	5.25	5.06	5.16
21j[c]	pGI_{50}	6.26	5.87	5.93	5.87	5.87	5.93	5.75	5.83	5.83	5.89
	pTGI	5.01	5.46	5.54	5.53	5.46	5.66	5.47	5.55	5.41	5.48
	pLC_{50}	–	5.09	5.15	5.26	5.11	5.09	5.19	5.26	5.05	5.11
22o[c]	pGI_{50}	6.65	6.02	6.48	6.00	6.18	6.26	6.08	6.29	6.53	6.25
	pTGI	6.29	5.65	6.09	5.67	5.82	5.86	5.71	5.97	6.17	5.87
	pLC_{50}	4.85	5.28	5.67	5.09	5.37	5.49	5.41	5.40	5.79	5.42
23o[c]	pGI_{50}	6.76	6.41	6.69	6.39	6.34	6.50	6.40	6.70	6.58	6.51
	pTGI	6.29	5.97	6.28	6.02	6.05	6.26	6.04	6.35	6.15	6.14
	pLC_{50}	5.35	5.43	5.90	5.42	5.65	5.90	5.58	5.98	5.53	5.67
24a	pGI_{50}	5.57	5.66	5.70	5.74	5.76	5.69	5.73	5.59	5.71	5.69
	pTGI	–	5.17	5.44	5.45	5.48	5.45	5.41	5.13	5.40	5.35
	pLC_{50}	–	4.18	4.61	5.25	5.26	–	4.62	4.14	4.25	4.33
25c[c]	pGI_{50}	6.09	5.50	5.71	5.71	5.68	5.65	5.71	5.75	5.77	5.71
	pTGI	4.49	5.06	5.21	5.35	5.31	5.31	5.36	5.49	5.36	5.22
	pLC_{50}	4.09	4.27	4.49	4.64	4.64	4.67	4.80	4.89	4.43	4.49
30a[c]	pGI_{50}	6.60	6.10	6.64	6.36	6.20	6.27	6.32	6.26	6.43	6.34
	pTGI	4.84	5.74	6.29	5.94	5.78	5.93	5.91	5.77	6.06	5.88
	pLC_{50}	–	5.29	5.82	5.65	5.53	5.46	5.90	5.34	5.69	5.42
30b	pGI_{50}	5.55	5.77	5.80	5.80	5.73	5.77	5.75	5.77	5.71	5.75
	pTGI	–	5.48	4.72	5.50	5.41	5.46	5.48	–	–	4.78
31a	pGI_{50}	5.06	–	4.46	4.07	4.04	4.38	–	–	4.03	4.20
34a	pGI_{50}	5.39	5.73	5.72	5.74	5.75	5.72	5.79	5.63	5.67	5.69
	pTGI	–	5.41	5.44	5.49	5.46	5.45	5.49	5.24	5.33	5.27
	pLC_{50}	–	4.92	4.48	4.91	5.24	4.81	5.21	4.56	4.59	4.71
35a	pGI_{50}	5.55	5.43	5.72	5.70	5.55	5.54	5.57	5.38	5.58	5.57
	pTGI	4.47	4.77	5.44	5.29	5.21	4.88	5.02	4.48	5.02	5.02
	pLC_{50}	–	4.01	4.94	4.94	4.63	4.40	4.50	4.21	4.34	4.39
Methyl-GAG[d]	pGI_{50}	5.10	4.60	4.90	4.70	4.40	4.80	4.70	4.00	4.80	4.67

[a] Highest conc. = 10^{-4} M unless otherwise reported; only modes showing a value >4.00 are reported.
[b] Mean Graph MID point i.e. the calculated mean panel.
[c] Mean of two separate experiments.
[d] Highest conc. = $10^{-4.3}$ M.

Table 4
Serine-Threonine kinase inhibition.

NSC	Compound	Ref.	Mean GI_{50} μM[a]	N. exp.	RSK2 Mean IC_{50} μM	N. Exp.	CHK1 Mean IC_{50} μM	N.exp.	CHK2 Mean IC_{50} μM
720135	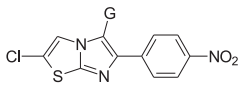 **36**	[15]	0.49	14	0.97	3	>100	7	78.75
748103	**23o**	–	0.31	2	1.23	1	>100	2	88.50
748105	**22o**	–	0.56	2	2.15	1	>100	2	56.50
720137	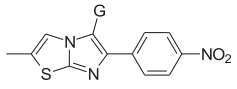 **37**	[15]	0.91	11	2.80	2	>100	8	83.00
734179	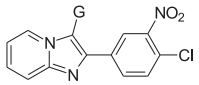 **38**	[2]	1.82	7	2.89	2	>100	6	79.00
709139	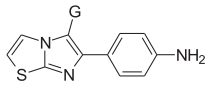 **39**	[14]	30.90	4	3.00	2	>100	6	67.50
709138	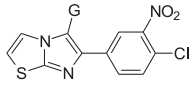 **40**	[14]	1.58	5	3.13	2	>100	2	81.00
725093	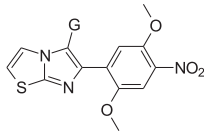 **41**	[3]	20.89	7	3.58	2	>100	4	96.00
720136	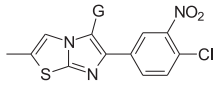 **42**	[15]	0.87	8	3.76	2	>100	7	64.80
747110	**17j**	–	1.35	3	3.93	3	>100	3	41.30
722870	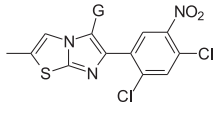 **43**	[17]	2.14	3	4.53	2	>100	3	>100
709136	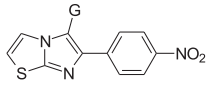 **44**	[14]	1.93	5	5.66	1	>100	3	>100
722868	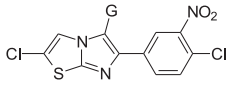 **45**	[15]	2.51	11	5.85	2	>100	5	90.00
720142	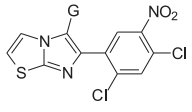 **46**	[17]	1.74	3	5.93	2	>100	3	>100

Table 4 (*continued*)

NSC	Compound	Ref.	Mean GI_{50} μM[a]	N. exp.	RSK2 Mean IC_{50} μM	N. Exp.	CHK1 Mean IC_{50} μM	N.exp.	CHK2 Mean IC_{50} μM
723550	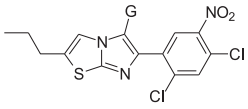 **47**	[17]	1.51	3	5.97	2	>100	3	>100
722874	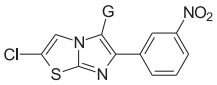 **48**	[15]	3.24	3	6.03	2	>100	3	>100
723549	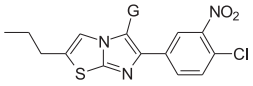 **49**	[15]	1.51	4	6.43	2	>100	4	90.50
732182	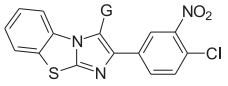 **50**	[2]	0.59	3	7.32			5	>100
745849	**34b**	–		2	7.80	1	>100	2	>100
745252	**17a**		2.04	5	8.26	1	>100	2	>100
748104	**17n**		1.07	2	8.55	1	>100	2	93.50
745255	**30b**		1.78	2	10.15	1	>100	2	>100
734184	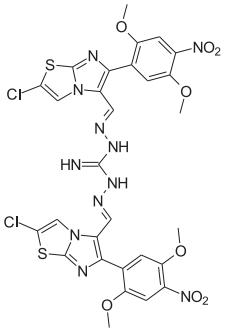 **51**	[2]	2.14	2	11.40	1	>100	2	>100
745256	**30a**	–	0.46	2	12.00	1	>100	2	>100
723551	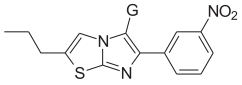 **52**	[15]	1.86	2	13.25	2	>100	4	69.50
720143	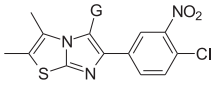 **53**	[15]	1.20	3	13.93	2	>100	4	48.50
698274	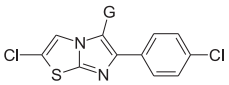 **54**	[18]	1.35	2	14.00	1	79.00	3	49.32
722871	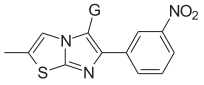 **55**	[15]	1.55	2	17.50	2	>100	4	59.00

(*continued on next page*)

Table 4 (*continued*)

NSC	Compound	Ref.	Mean GI_{50} μM[a]	N. exp.	RSK2 Mean IC_{50} μM	N. Exp.	CHK1 Mean IC_{50} μM	N.exp.	CHK2 Mean IC_{50} μM
730326	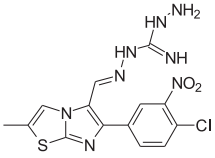 **56**	[2]	1.70	2	18.00	1	>100	2	>100
722875	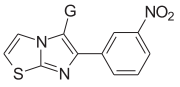 **57**	[15]	5.01	2	18.50	2	>100	3	>100
730327	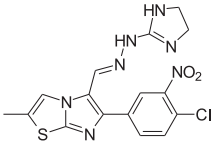 **58**	[2]	1.26	2	20.50	1	>100	2	>100
723552	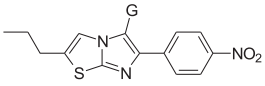 **59**	[15]	1.58	4	20.95	2	>100	5	>100
732180	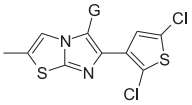 **60**	[2]	1.10	2	26.50	1	>100	2	>100
747108	**21j**	–	1.66	3	30.67	2	78.50	2	18.85
720138	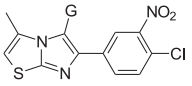 **61**	[15]	1.41	6	44.80	2	>100	7	84.40
747112	**20j**	–	2.09	4	53.75	1	>100	2	77.50
747420	**20m**	–	1.20	3	56.73	1	>100	3	>100
732181	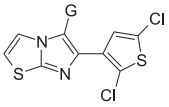 **62**	[2]	1.62	3	79.00	1	>100	3	65.00
723553	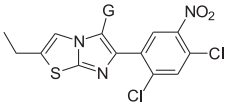 **63**	[17]	1.48	3	83.00	1	>20	1	59.00
747109	**17e**	–	1.41	2	86.00	2	>100	1	90.00
734178	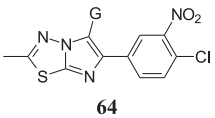 **64**	[2]	1.26	1	94.00			2	78.00

Table 4 (*continued*)

NSC	Compound	Ref.	Mean GI_{50} μM[a]	N. exp.	RSK2 Mean IC_{50} μM	N. Exp.	CHK1 Mean IC_{50} μM	N.exp.	CHK2 Mean IC_{50} μM
722877	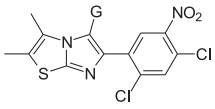 **65**	[17]	6.31	2	98.50			1	>100
726886	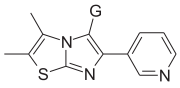 **66**	[17]	–	2	>100	3	>100	6	6,58
728902	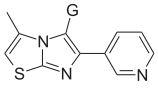 **67**	[17]	–	2	>100	3	>100	6	34,32
745254	**18a**	–	2.34	1	>100			1	>20
745257	**34a**	–	2.04	2	>100			1	>20
745253	**18b**	–	–	1	>100			1	>20
745258	**25c**	–	1.95	1	>100			1	>20
745850	**24a**	–	2.04	1	>100			1	>20
745851	**31a**	–	63.10	1	>100			1	>100
745852	**35a**	–	2.69	1	>100			1	>20
747111	**20e**	–	2.45	2	>100	1	>100	1	>100
747415	**20f**	–	–	1	>100			1	>100
747413	**20g**	–	–	1	>100			1	>100
747414	**20h**	–	1.78	1	>100			1	>100
747419	**20i**	–	1.95	1	>100			1	>100
747421	**20k**	–	2.00	1	>100			1	>100
747417	**20l**	–	2.04	1	>100			1	>100
747107	**21e**	–	1.66	2	>100	1	>100	1	>50
747418	**17d**	–	5.25	1	>100			1	>100

Compounds ordered by decreasing RSK2 activity. Those with structural formula were reported in previous papers.
G stays for CH=N–NH–C(NH)NH_2 (all the compounds are hydrochlorides, except the hydrobromides reported in Table 1 and **58**).
[a] When this value is missing, the compound was not tested.

Compound **20l**, bearing at the 6 position a *m*-trifluoromethylphenyl group, showed about the same activity of the 6-*p*-fluorophenyl derivative **20e** (mean pGI_{50} 5.69 and 5.61 respectively). As noticed in the previous papers, an appropriate substituent at the 2 position of the imidazothiazole system is important for a potent activity (see **17e,j** and **21e,j**).

- The effect of replacing fluorine by bromine in the nitrophenyl derivatives, is shown by comparison of the fluoro derivative **20j** (mean pGI_{50} 5.68) with the bromo derivative **20m** (mean pGI_{50} 5.92). Among the halogens considered (the corresponding chloro derivative showed mean pGI_{50} 5.77 [14]) bromine seems the most suitable.

Shifting the halogen from the phenyl to the thiazole ring (compound **22o** and **23o**) leads to compounds which are among the most active described in this paper with mean pGI_{50} 6.25, 6.51 respectively (6.31 for the 2-chloro derivative previously published [15]).

- The introduction of an electron donating group at position 2 (**19d**) was detrimental.

Among the 2-chloro-imidazothiazoles, the activity of compounds **17d** and **17n** confirms that the introduction of electron attracting groups in the phenyl ring is useful (chlorine showed mean pGI_{50} 5.87, fluorine 5.85, *p*-nitro 6.31, *m*-nitro 5.49, cyano 5.97 vs. 5.28 for the unsubstituted phenyl ring).

Table 5
Kinase inhibition of compound **23o**.

	Compounds IC_{50} (nM)[a]			
	Dasatinib NSC 732517	Sunitinib NSC 736511	**23o** NSC 748103	Staurosporine
Serine-Threonine Kinases				
Aurora A	2633.00	1837.00	>20,*000*	0.60
CHK1		77.27	13820.00	<0.5
CHK2		16.84	1960.00	3.34
RSK1	>20,*000*	131.30	1181.00	<0.5
RSK2	>20,*000*	183.90	607.10	<0.5
Tyrosine Kinases				
ALK		54.64	>20,*000*	2.36
cMET		>20,*000*		404.90
c-Src	<1	152.80		0.83
LCK	<1	8.90		1.33
ZAP70				8.63

[a] Empty cells indicate no inhibition or compound activity that could not be fit to an IC_{50} curve.

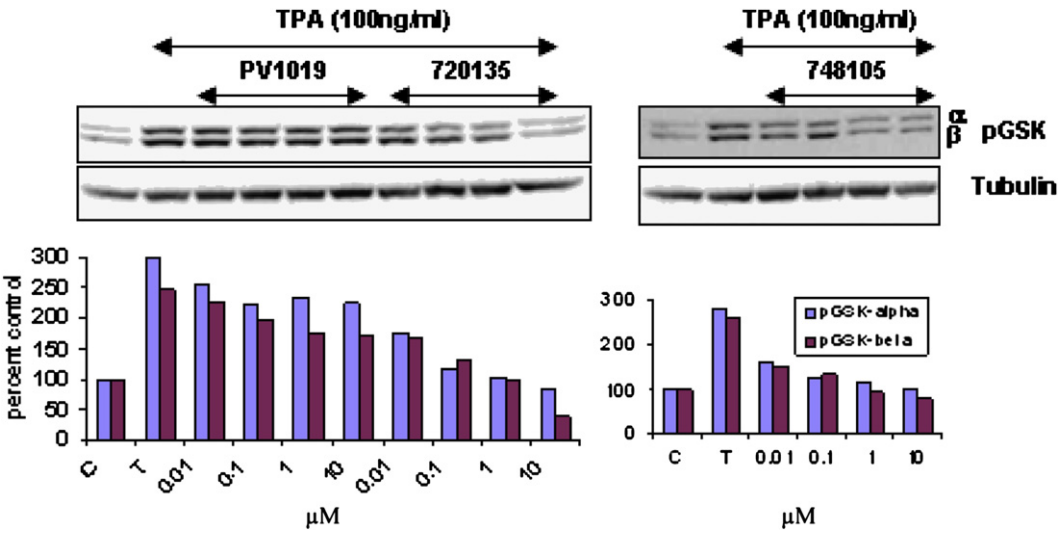

Fig. 1. MCF-7 cells were serum starved overnight, pretreated with indicated inhibitors [**22o** (NSC 748105), **36** (NSC 720135) and PV1019] for 30 min and stimulated with vehicle or TPA (100 ng/ml) for 15 min. Proteins extracted were immunoblotted for GSK3 α/β and tubulin. The densities were measured using Syngene software and ratio between GSK3 and tubulin calculated, plotted as percent control.

3.2. RSK2 kinase inhibition

Compounds were screened for inhibition of RSK2 kinase using the high-throughput, non-radioactive method described previously [16].

Kinase inhibition values and tumor growth inhibition expressed as micromolar concentration are listed in Table 4. To assess the selectivity of the kinase inhibition, we initially examined the compounds in analogous non-radioactive assays addressing CHK1, CHK2, and Aurora kinases. No inhibition was observed at concentrations up to 100 μM for Aurora kinase, therefore are not reported in the table.

3.2.1. Relationship between RSK2 kinase inhibition and tumor cell growth inhibition in the NC-I60

A substantial range in potency for inhibition of RSK2 was observed in this series of compounds. Numerous compounds showed potency as growth inhibitors without appreciable potency as RSK2 inhibitors. Two compounds (**39**, **41**) were potent RSK2 inhibitors without appreciable activity as growth inhibitors. The less than perfect correlation observed between the two activities, and lack of closely coherent COMPARE analysis (data not shown), suggest that even within this subset of compounds, multiple mechanisms of action contribute to the observed growth inhibition. The three most potent RSK2 inhibitors **36** (NSC 720135) together with the F (**22o**) and Br (**23o**) variants showed even greater potency for tumor cell growth inhibition at the GI_{50} level of effect. This could be due to transport across cell membranes resulting in increased intracellular concentrations of these compounds or may simply reflect the critical nature of RSK2 for tumor cell growth.

3.2.2. Kinase selectivity of RSK2 inhibitors

One of the most potent RSK2 inhibitors (**23o** NSC 748103) was then profiled for inhibition of a panel of Serine-Threonine and Tyrosine kinases using a radioactive assay (testing conducted by Reaction Biology, Inc., Malvern, PA). As indicated in Table 5, **23o** did not inhibit any of the tyrosine kinases and showed approximately two fold greater potency against RSK2 than the very closely related RSK1 enzyme. Some activity was observed for CHK2 and, to a lesser extent CHK1 kinase. No activity was observed, up to 20,000 nM, for Aurora A kinase. The validity of these profiling results was supported by the results for a highly selective tyrosine kinase inhibitor (Dasatinib) and broad spectrum inhibitors (Sunitinib and Staurosporine) which were profiled concurrently.

3.3. Cell-based assays

3.3.1. Effect of RSK2 inhibitors on cell proliferation of MCF-7 and MCF-10A cells

To evaluate the specificity of some of the most potent RSK inhibitors in cell-based assays we analyzed their ability to preferentially inhibit the growth of the human breast cancer line, MCF-7, compared to the normal human breast line, MCF-10A. We have previously validated this differential growth assay as a method for analyzing the specificity of RSK inhibitors [8,19]. The cells were treated with the inhibitors (**22o**, **23o**, **37**, **40** and **45**) at various concentrations and cell viability was measured after 48 h of exposure. Compounds **40**, **45** and **22o** preferentially inhibited the growth of the human breast cancer line, MCF-7, but did not inhibit the growth of the non-transformed mammary line, MCF-10A; compound **22o** has the lowest IC_{50} of this group, compounds **37** and **23o** inhibited the growth of both cell lines (data not shown).

3.3.2. GSK3 α/β as a biomarker for RSK2 inhibition

RSKs are serine/threonine kinases that are activated by signaling inputs from ERK1/2 and PDK1. RSK specificity for target phosphorylation has been determined using synthetic peptide libraries and was determined that RSK prefers to phosphorylate Ser residues on the substrates [20]. This result has enabled identification of possible RSK functions in transcription and translational regulation, cell growth, motility, proliferation and survival [21]. Many of the substrates identified so far could be phosphorylated by one or more isoforms of RSKs and several RSK2 substrates reported in the literature were evaluated as possible biomarkers for RSK2 inhibitors. RSK substrates such as BAD (s112) Histone H3 (s10), ATF4 and CREB were screened but none of them gave consistent data across the cell lines examined [9].

Treatment of cells with 12-o-tetradecanoylphorbol-13-acetate (TPA) is known to result in activation of ERK1/2 and RSKs. Activated RSK in turn results in phosphorylation of both GSK isoforms. Sapkota et al. also showed that the RSK inhibitor BI-D1870 inhibited GSK3 in HEK 293 cells at 10 μM. The inhibition of the

phosphorylation of GSK3 α (S21)/β (S9) was confirmed also in MCF-7 and T47D cell lines [9]. We chose to measure the phosphorylation status of the ATF4, CREB (Transcriptional regulation), BAD (survival and apoptosis) and GSK3 α/β (proliferation and metabolism) in the presence or absence of the compound under test to determine if one of them could be useful as a possible biomarker for RSK2 inhibitors. In the cell lines we evaluated, ATF4, CREB, BAD did not give consistent results and the bands were weak making them difficult to analyze (data not shown), whereas, the immunoblots with GSK3 α/β were consistent and clear.

The Fig. 1 presents the data obtained using MCF-7 cells; TPA treatment increased GSK phosphorylation to twice the control level. Pre-treatment of cells for 30 min with **22o** (NSC 748105) and **36** (NSC 720135) was enough to inhibit TPA (100 ng/mL for 15 min) induced GSK3 α/β phosphorylation by 50% at concentrations as low as 10 nM. A structurally similar compound, PV1019 shares guanadinylhydrazone moiety, is a potent and selective inhibitor of CHK2 with chemotherapeutic and radiosensitization potential related CHK2 inhibitor [22], did not inhibit phosphorylation of GSK3.

4. Conclusion

We designed and synthesized a new series of imidazo[2,1-*b*] thiazole guanylhydrazones which were tested as cytotoxic agents and as RSK2 inhibitors. The results were compared with previously described analogs. A small subset of compounds showed both potent inhibition of RSK2 kinase activity and tumor cell growth in vitro. Detailed study of the most active compounds (**22o**, **23o** and the previously reported 2-chloro analog **36**) indicates a high degree of selectivity for inhibition of RSK2 kinase compared to a spectrum of other related kinases. Selective inhibition of the MCF-7 breast tumor cell line compared to MCF-10A non-transformed cells, as well as selective inhibition of the biomarker GSK3 provides evidence that the compounds can affect the RSK2 target in cells. These compounds may serve as useful leads for development of novel therapeutics intervening in the growth and metastasis of tumor cells.

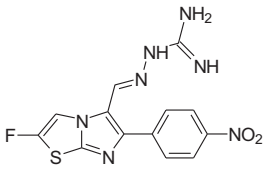

22o

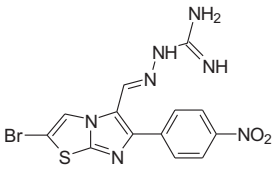

23o

5. Experimental section (see also Supplementary data)

5.1. Chemistry

All the compounds prepared have a purity of at least 95% as determined by combustion analysis.

The melting points are uncorrected. TLC was performed on Fluka plates (art. 99577) and the eluent was a mixture of petroleum ether/acetone in various proportions. The IR spectra were recorded in nujol on a Nicolet Avatar 320 E.S.P.; ν_{max} is expressed in cm^{-1}. The ^1H NMR spectra were recorded on a Varian Gemini (300 MHz); the chemical shift (referenced to solvent signal) is expressed in δ (ppm) and J in Hz (abbreviations: ar = aromatic, bzt = benzothiazole, ex = H linked to N which exchanged with D_2O, im = imidazole, py = pyridine, th = thiazole, thio = thiophene). For the spectra which are not reported here see Supplementary data, Table S1.

The starting compounds **1** (2-amino-5-chlorothiazole, 2-amino-5-bromothiazole, 2-amino-5-fluorothiazole, 2-amino-5-methylthiazole, 2-amino-5-methylthiadiazole, or 2,5-diaminothiadiazole, see Tables 1 and 2), **2a**–**i**,**l**–**o**, **26** and **27** are commercially available. Compounds **5d**, **6e**, **10d**, **11c** and **13l** were prepared according to the literature [2,10–13].

5.1.1. Synthesis of the 2-bromo-3′-nitroacetophenones (*2j*,*k*) (Scheme 1)

The appropriate 2-bromoacetophenone (10 mmol) was added portionwise to stirred fuming nitric acid (15 mL), at 0 °C. The reaction mixture was stirred for 1 h at this temperature and poured onto ice. The resulting solid product was collected by filtration, with a yield of 70–85%, and subjected to the following reaction without further purification.

2j. $C_8H_5BrFNO_3$ MW 262.03, mp 63–65 °C (petroleum ether). IR: 1701, 1609, 1532, 1086, 835. ^1H NMR: 5.05 (2H, s, CH_2), 7.81 (1H, m, ar), 8.41 (1H, m, ar), 8.68 (1H, m, ar). Anal. $C_8H_5BrFNO_3$ (C, H, N).

2k. $C_8H_5BrFNO_3$ MW 262.03, mp 58–61 °C (EtOH). IR: 1701, 1624, 1527, 1081, 835. ^1H NMR: 4.95 (2H, s, CH_2), 7.71 (1H, t, ar, J = 9.5), 8.54 (1H, m, ar), 8.67 (1H, m, ar). Anal. $C_8H_5BrFNO_3$ (C, H, N).

5.1.2. Synthesis of the compounds *3a*,*e*,*j*,*n*, *4a*,*b*, *6f*–*k*,*m*, *7e*,*j*, *8o*, *9o* (Scheme 1), *28a*,*b*, *32a*,*b* (Scheme 2)

The appropriate 2-amino-derivative (**1**, **26**, **27**) (20 mmol) was dissolved in 100 mL of acetone and treated with an equivalent of the appropriate 2-bromoacetylderivative **2**. The reaction mixture was refluxed for 1–5 h (according to a TLC test). Compounds **3a**, **4b**, **28b**, **32a**,**b** were separated from the acetone solution as hydrobromides and the free bases were prepared. In all the other cases, the reaction mixture was cooled, the solid product was separated by filtration and the resulting intermediate salt ($\nu_{C=O}$ absorption was confirmed around 1700 cm^{-1}) was used in the subsequent step without further purification. It was refluxed for 1–4 h with 200 mL of 2N HCl and, before complete cooling, the solution was cautiously basified by dropwise addition of 15% NH_4OH. The solid product obtained was collected by filtration. All the derivatives were crystallized from ethanol except **32b** (chloroform/petroleum ether), with a yield of 23% (**28b**), 35–60% (**3a**, **4a**,**b**, **6f**–**k**,**m**, **7e**,**j**, **28a**, **32a**,**b**;) and 70–85% (**3e**,**j**,**n**, **8o**, **9o**).

5.1.3. Synthesis of the aldehydes *10a*,*e*,*j*,*n*, *11a*,*b*, *12d*, *13e*–*k*,*m*, *14e*,*j*, *15o*, *16o* (Scheme 1) and *29a*,*b*, *33a*,*b* (Scheme 2)

The Vilsmeier reagent was prepared at 0–5 °C by dropping $POCl_3$ (54 mmol) into a stirred solution of DMF (65 mmol) in $CHCl_3$ (5 mL). The appropriate condensed imidazole system (5 mmol) was suspended in $CHCl_3$ (20 mL). The mixture thus obtained was dropped into the Vilsmeier reagent while maintaining stirring and cooling. The reaction mixture was kept for 3 h at room temperature and under reflux for 15–20 h (according to a TLC test). Chloroform was removed under reduced pressure and the resulting oil was poured onto ice. The crude precipitated aldehydes (in the case of **10j** and **13g** it was necessary to basify the aqueous solution with 15% NH_4OH to induce precipitation) were collected by filtration and crystallized from chloroform/petroleum ether (**10a**, **11a**,**b**, **29a**,**b**, **33a**,**b**) or ethanol (**10e**,**j**,**n**, **12d**, **13e**–**k**,**m**, **14e**,**j**, **15o**, **16o**), with a yield of 60–70% (**10e**,**j**,**n**, **13e**–**k**,**m**, **15o**, **33a**) and 80–95% (**10a**, **11a**,**b**, **12d**, **14e**,**j**, **16o**, **29a**,**b**, **33b**).

5.1.4. Synthesis of the hydrazones *17*–*25* (Scheme 1) and *30*, *31*, *34*, *35* (Scheme 2)

The appropriate aldehyde (10 mmol) was dissolved in ethanol and treated with an equivalent of the appropriate hydrazine:

- aminoguanidine hydrochloride for compounds **17a**,**d**,**e**,**j**,**n**, **18a**,**b**, **19d**, **20e**–**m**, **21e**,**j**, **22o**, **23o**, **30a**,**b**, **34a**,**b**.
- 2-hydrazino-2-imidazoline hydrobromide for compounds **24a**, **25c**, **31a** and **35a**.

The reaction mixture was refluxed for 5–20 h according to a TLC test, and the resulting precipitate, obtained from the reaction mixture or after partial solvent evaporation, was collected by filtration with a yield of 50–60% (**17d**,**e**,**j**, **19d**, **20e**,**f**,**h**,**i**,**k**–**m**, **22o**, **24a**, **25c**, **30b**, **31a**, **34a**, **35a**), 70–80% (**17a**,**n**, **18a**, **20g**,**j**, **21e**,**j**, **23o**, **34b**), and 85–95% (**18b**, **30a**). In the case of compound **34a** diethyl ether was added to the ethanol solution to induce crystallization.

17a. IR: 3305, 3140, 1686, 1231, 835. ^{1}H NMR: 7.36 (1H, s, thio), 7.79 (4H, broad, ex), 8.22 (1H, s, th), 8.91 (1H, s, CH), 11.89 (1H, s, ex). Anal. $C_{11}H_7Cl_3N_6S_2HCl$ (C, H, N).

17d. IR: 3283–3022, 1670, 1158, 974. ^{1}H NMR: 7.47 (3H, m, ar), 7.67 (2H, m, ar), 8.48 (1H, s, th), 8.78 (4H, broad, ex), 8.90 (1H, s, CH), 12.13 (1H, s, ex). Anal. $C_{13}H_{11}ClN_6S\cdot HCl$ (C, H, N).

17e. IR: 3416–3022, 1675, 1168, 856. ^{1}H NMR: 7.34 (2H, m, ar), 7.59 (1H, broad, ex), 7.73 (2H, m, ar), 8.10 (3H, broad, ex), 8.45 (1H, s, th), 8.90 (1H, s, CH), 12.02 (1H, s, ex). Anal. $C_{13}H_{10}ClFN_6S\cdot HCl$ (C, H, N).

17j. IR: 3478–3160, 1696, 1163, 825. ^{1}H NMR: 7.70 (1H, m, ar), 7.90 (4H, broad, ex), 8.06 (1H, m, ar), 8.35 (1H, m, ar), 8.49 (1H, s, th), 8.85 (1H, s, CH), 12.01 (1H, s, ex). Anal. $C_{13}H_9ClFN_7O_2S\cdot HCl$ (C, H, N).

17n. IR: 3457–3129, 2233, 1680, 835. ^{1}H NMR: 7.82 (4H, broad, ex), 7.89 (2H, d, ar, $J = 8.1$), 7.97 (2H, d, ar, $J = 8.1$), 8.51 (1H, s, th), 8.90 (1H, s, CH), 11.94 (1H, s, ex). Anal. $C_{14}H_{10}ClN_7S\cdot HCl$ (C, H, N).

18a. IR: 3428–3154, 1685, 1647, 1150. ^{1}H NMR: 2.82 (3H, s, CH_3), 7.39 (1H, s, thio), 7.63 (4H, broad, ex), 8.33 (1H, s, CH), 12.12 (1H, s, ex). Anal. $C_{11}H_9Cl_2N_7S_2\cdot HCl$ (C, H, N).

20e. IR: 3288, 3124, 1680, 1158, 840. ^{1}H NMR: 7.34 (2H, m, ar), 7.57 (1H, d, th, $J = 4.4$), 7.73 (2H, m, ar), 7.84 (4H, broad, ex), 8.47 (1H, s, CH), 8.74 (1H, d, th, $J = 4.4$), 12.23 (1H, s, ex). Anal. $C_{13}H_{11}FN_6S\cdot HCl$ (C, H, N).

20h. IR: 3324–3000, 1680, 1153, 820. ^{1}H NMR: 7.56 (2H, m, ar + th), 7.75 (2H, m, ar), 7.80 (4H, broad, ex), 8.49 (1H, s, CH), 8.70 (1H, d, th, $J = 4.4$), 12.13 (1H, s, ex). Anal. $C_{13}H_{10}F_2N_6S\cdot HCl$ (C, H, N).

20i. IR: 3488–3114, 1680, 1061, 799. ^{1}H NMR: 7.57 (1H, d, th, $J = 4.2$), 7.78 (6H, m, 2ar + 4ex), 8.23 (1H, s, CH), 8.70 (1H, d, th, $J = 4.2$), 12.00 (1H, s, ex). Anal. $C_{13}H_9F_3N_6S\cdot HCl$ (C, H, N).

20j. IR: 3442–3124, 1685, 1168, 851. ^{1}H NMR: 7.55 (1H, d, th, $J = 4.3$), 7.72 (1H, m, ar), 7.80 (4H, broad, ex), 8.10 (1H, m, ar), 8.39 (1H, m, ar), 8.54 (1H, s, CH), 8.68 (1H, d, th, $J = 4.3$), 12.05 (1H, s, ex). Anal. $C_{13}H_{10}FN_7O_2S\cdot HCl$ (C, H, N).

20k. IR: 3473–3094, 1680, 1061, 840. ^{1}H NMR: 7.59 (1H, d, th, $J = 4.6$), 7.71 (1H, m, ar), 7.78 (4H, broad, ex), 8.29 (1H, s, CH), 8.38 (1H, m, ar), 8.48 (1H, m, ar), 8.70 (1H, d, th, $J = 4.6$), 12.05 (1H, s, ex). Anal. $C_{13}H_{10}FN_7O_2S\cdot HCl$ (C, H, N).

20l. IR: 3450–3109, 1737, 1173, 861. ^{1}H NMR: 6.84 (4H, broad, ex), 7.56 (1H, d, th, $J = 4.4$), 7.73 (3H, m, ar), 7.99 (1H, m, ar), 8.52 (1H, s, CH), 8.73 (1H, d, th, $J = 4.4$), 12.17 (1H, s, ex). Anal. $C_{14}H_{11}F_3N_6S\cdot HCl$ (C, H, N).

20m. IR: 3565–3119, 1624, 1030, 825. ^{1}H NMR: 7.54 (1H, d, th, $J = 4.5$), 7.80 (4H, broad, ex), 7.90 (1H, dd, ar-6, $J = 8.4$, $J = 2.1$), 7.99 (1H, d, ar-5, $J = 8.4$), 8.29 (1H, d, ar-2, $J = 2.1$), 8.54 (1H, s, CH), 8.67 (1H, d, th, $J = 4.5$), 11.96 (1H, s, ex). Anal. $C_{13}H_{10}BrN_7O_2S\cdot HCl$ (C, H, N).

21e. IR: 3252, 1675, 1235, 1168, 846. ^{1}H NMR: 2.52 (3H, d, CH_3, $J = 1.3$), 7.34 (2H, m, ar), 7.72 (2H, m, ar), 7.80 (4H, broad, ex), 8.44 (1H, s, CH), 8.47 (1H, d, th, $J = 1.3$), 12.12 (1H, s, ex). Anal. $C_{14}H_{13}FN_6S\cdot HCl$ (C, H, N).

21j. IR: 3500–3000, 1680, 1168, 912. ^{1}H NMR: 2.52 (3H, d, CH_3, $J = 1.5$), 7.71 (1H, m, ar), 7.74 (4H, broad, ex), 8.09 (1H, m, ar), 8.37 (1H, m, ar), 8.43 (1H, d, th, $J = 1.5$), 8.49 (1H, s, CH), 11.96 (1H, s, ex). Anal. $C_{14}H_{12}FN_7O_2S\cdot HCl$ (C, H, N).

22o. IR: 3462–3135, 1696, 1214, 851. ^{1}H NMR: 7.78 (4H, broad, ex), 7.98 (2H, d, ar, $J = 8.7$), 8.33 (2H, d, ar, $J = 8.7$), 8.56 (1H, s, th), 8.87 (1H, s, CH), 12.02 (1H, broad, ex). Anal. $C_{13}H_{10}FN_7O_2S\cdot HCl$ (C, H, N).

23o. IR: 3467–3135, 1634, 1163, 861. ^{1}H NMR: 7.81 (4H, broad, ex), 7.95 (2H, d, ar, $J = 8.7$), 8.29 (2H, d, ar, $J = 8.7$), 8.56 (1H, s, th), 8.87 (1H, s, CH), 12.11 (1H, s, ex). Anal. $C_{13}H_{10}BrN_7O_2S\cdot HCl$ (C, H, N).

24a. IR: 3309–3170, 1675, 1240, 1030. ^{1}H NMR: 3.77 (4H, s, 2× CH_2), 7.37 (1H, s, thio), 8.22 (1H, s, th), 8.41 (2H, broad, ex), 8.85 (1H, s, CH), 12.23 (1H, broad, ex). Anal. $C_{13}H_9Cl_3N_6S_2\cdot HBr$ (C, H, N).

25c. IR: 3580–3186, 1681, 1076, 897. ^{1}H NMR: 2.82 (3H, s, CH_3), 3.74 (4H, s, 2× CH_2), 7.88 (1H, d, ar-5, $J = 8.4$), 8.24 (1H, dd, ar-6, $J = 8.4$, $J = 2$), 8.35 (3H, broad, ex), 8.57 (1H, s, CH), 8.68 (1H, d, ar-2, $J = 2$). Anal. $C_{15}H_{13}ClN_8O_2S\cdot HBr$ (C, H, N).

30a. IR: 3469, 3105, 1682, 1637, 838. ^{1}H NMR: 7.41 (1H, s, thio), 7.50 (1H, td, bzt, $J = 7.6$, $J = 1.8$), 7.57 (1H, td, bzt, $J = 7.6$, $J = 1.8$), 7.77 (4H, broad, ex), 8.13 (1H, dd, bzt, $J = 7.6$, $J = 1.8$), 8.41 (1H, s, CH), 8.68 (1H, dd, bzt, $J = 7.6$, $J = 1.8$), 12.03 (1H, s, ex). Anal. $C_{15}H_{10}Cl_2N_6S_2\cdot HCl$ (C, H, N).

30b. IR: 3490–3148, 1670, 1220, 1034. ^{1}H NMR: 3.82 (3H, s, OCH_3), 3.92 (3H, s, OCH_3), 7.46 (1H, s, ar), 7.50 (1H, t, bzt, $J = 7.7$), 7.56 (1H, t, bzt, $J = 7.7$), 7.70 (4H, broad, ex), 7.72 (1H, s, ar), 8.12 (1H, d, bzt, $J = 7.7$), 8.34 (1H, s, CH), 8.69 (1H, d, bzt, $J = 7.7$), 12.08 (1H, s, ex). Anal. $C_{19}H_{17}N_7O_4S\cdot HCl$ (C, H, N).

3**1a**. IR: 3580–3078, 1669, 1235, 933. ^{1}H NMR: 3.76 (4H, s, 2× CH_2), 7.41 (1H, s, thio), 7.56 (2H, m, bzt), 8.14 (1H, dd, bzt, $J = 8.1$, $J = 1.2$), 8.36 (1H, s, CH), 8.59 (2H, s, ex), 8.76 (1H, dd, bzt, $J = 8.1$, $J = 1.2$), 12.41 (1H, broad, ex). Anal. $C_{17}H_{12}Cl_2N_6S_2\cdot HBr$ (C, H, N).

34a. IR: 3298–3064, 1673, 1192, 888. ^{1}H NMR: 7.30 (1H, t, py, $J = 7.6$), 7.45 (1H, s, thio), 7.71 (1H, t, py, $J = 7.6$), 7.82 (4H, broad, ex), 7.88 (1H, d, py, $J = 7.6$), 8.40 (1H, s, CH), 9.58 (1H, d, py, $J = 7.6$), 12.05 (1H, s, ex). Anal. $C_{13}H_{10}Cl_2N_6S\cdot HCl$ (C, H, N).

35a. IR: 3575–3032, 1677, 1256, 1035. ^{1}H NMR: 3.77 (4H, s, 2× CH_2), 7.23 (1H, t, py, $J = 7.6$), 7.43 (1H, s, thio), 7.62 (1H, t, py, $J = 7.6$), 7.83 (1H, d, py, $J = 7.6$), 8.39 (1H, s, CH), 8.56 (2H, broad, ex), 9.52 (1H, d, py, $J = 7.6$), 12.20 (1H, broad, ex). Anal. $C_{15}H_{12}Cl_2N_6S\cdot HBr$ (C, H, N).

5.2. Biology

5.2.1. Cell-based screening assay

The NCI screening is a two stage process [23], beginning with the evaluation of all compounds against the 60 cell lines at a single concentration of 10^{-5} M. Compounds exhibiting significant growth inhibition were evaluated against the 60 cell panel at five concentration levels by the NCI according to standard procedures (http://dtp.nci.nih.gov/branches/btb/ivclsp.html). In both cases the exposure time was 48 h.

5.2.2. High-throughput kinase assay methodology

High-throughput assays for kinase inhibition were conducted in 384-well plates and utilized IMAP technology (Molecular Devices, Inc.). In brief, recombinant kinase (RSK1, RSK2, CHK1, CHK2, or Aurora A) was incubated with fluorescent peptide substrate in buffer containing 10 μM ATP. Phosphorylated peptide was then bound to IMAP beads which resulted in an increase in the polarization signal which was read on a Tecan Ultra microplate reader. Data were normalized to control values and concentrations effective in inhibiting kinase activity by 50% (IC_{50}) were read from concentration response curves by linear interpolation.

5.2.3. Cell culture and immunoblotting

MCF-7, MCF-10A, T47D and HEK 293 cells were obtained from ATCC and cultured and maintained in RPMI medium supplemented

with 10% FBS and antimycotic/antibiotic solution (Invitrogen, Gaithersburg, MD). Cells at 70–80% confluence were serum starved overnight and pretreated for 30 min with the inhibitors. The cells were stimulated with or without TPA (400 ng/mL) for 20 min respectively. The cells were washed twice with ice cold PBS and lysed in ice cold lysis buffer to extract total proteins, incubated on ice for 15 min and samples were centrifuged at 16,000 rpm at 4 °C and clear supernatant is collected. The samples were used immediately or stored at −80 °C until use. Protein concentrations were measured using PIERCE kit (Thermo Scientific, Rockford, IL). Fifty μg of each protein sample was separated using SDS/PAGE and transferred on to PVDF membranes. The membranes were probed with various antibodies (Cell signaling technologies, Cambridge, MA) using the standard protocols. Proteins were detected using HRP conjugated secondary antibodies and ECL plus reagents (GE healthcare, Pittsburgh, PA). The images are captured and densitometric analysis was carried out by using Syngene (Syngene, Frederick, MD) software.

For proliferation studies MCF-7 and MCF-10A cells were seeded at 2500–5000 cells per well in 96 well tissue culture plates in the appropriate medium. After 24 h, the medium was replaced with medium containing compound or vehicle as indicated. Cell viability was measured at indicated time points using CellTiter-Glo assay reagent (Promega, Madison, WI) according to the manufacturer's protocol.

Acknowledgment

This work has been supported by a grant from the University of Bologna and by the Developmental Therapeutics Program of the Division of Cancer Treatment of the National Cancer Institute.

Appendix. Supplementary data

Supplementary data related to this article can be found online at doi:10.1016/j.ejmech.2011.07.001.

References

[1] Potential Antitumor Agents. 47. For part 46 see the following: A. Andreani, S. Bellini, S. Burnelli, M. Granaiola, A. Leoni, A. Locatelli, R. Morigi, M. Rambaldi, L. Varoli, N. Calonghi, C. Cappadone, M. Zini, C. Stefanelli, L. Masotti, R.H. Shoemaker, Substituted *E*-3-(3-indolylmethylene)-1,3-dihydroindol-2-ones with antitumor activity. In depth study of the effect on growth of breast cancer cells, J. Med. Chem. 53 (2010) 5567–5575.

[2] A. Andreani, S. Burnelli, M. Granaiola, A. Leoni, A. Locatelli, R. Morigi, M. Rambaldi, L. Varoli, N. Calonghi, C. Cappadone, G. Farruggia, M. Zini, C. Stefanelli, L. Masotti, N.S. Radin, R.H. Shoemaker, New antitumor imidazo [2,1-*b*]thiazole guanylhydrazones and analogues, J. Med. Chem. 51 (2008) 809–816.

[3] A. Andreani, M. Granaiola, A. Leoni, A. Locatelli, R. Morigi, M. Rambaldi, G. Lenaz, R. Fato, C. Bergamini, G. Farruggia, Potential antitumor agents. 37. Synthesis and antitumor activity of guanylhydrazones from imidazo[2,1-*b*] thiazoles and from the new heterocyclic system thiazolo[2′,3′:2,3]imidazo [4,5-*c*]quinoline, J. Med. Chem. 48 (2005) 3085–3089.

[4] K. Müller, C. Faeh, F. Diederich, Fluorine in pharmaceuticals: looking beyond intuition, Science 317 (2007) 1881–1886.

[5] A.G. Jobson, J.H. Cardellina 2nd, D. Scudiero, S. Kondapaka, H. Zhang, H. Kim, R. Shoemaker, Y. Pommier, Identification of a bis-guanylhydrazone [4,4′-diacetyldiphenylurea-bis(guanylhydrazone); NSC 109555] as a novel chemotype for inhibition of Chk2 kinase, Mol. Pharmacol. 72 (2007) 876–884.

[6] C.E. Poteet-Smith, J.A. Smith, D.A. Lannigan, T.A. Freed, T.W. Sturgill, Generation of constitutively active p90 ribosomal S6 kinase in vivo. Implications for the mitogen-activated protein kinase-activated protein kinase family, J. Biol. Chem. 274 (1999) 22135–22138.

[7] U. Doehn, C. Hauge, S.R. Frank, C.J. Jensen, K. Duda, J.V. Nielsen, M.S. Cohen, J.V. Johansen, B.R. Winther, L.R. Lund, O. Winther, J. Taunton, S.H. Hansen, M. Frödin, RSK is a principal effector of the RAS-ERK pathway for eliciting a coordinate promotile/invasive gene program and phenotype in epithelial cells, Mol. Cell. 35 (2009) 511–522.

[8] J.A. Smith, C.E. Poteet-Smith, Y. Xu, T.M. Errington, S.M. Hecht, D.A. Lannigan, Identification of the first specific inhibitor of p90 ribosomal S6 kinase (RSK) reveals an unexpected role for RSK in cancer cell proliferation, Cancer Res. 65 (2005) 1027–1034.

[9] G.P. Sapkota, L. Cummings, F.S. Newell, C. Armstrong, J. Bain, M. Frodin, M. Grauert, M. Hoffmann, G. Schnapp, M. Steegmaier, P. Cohen, D.R. Alessi, BI-D1870 is a specific inhibitor of the p90 RSK (ribosomal S6 kinase) isoforms in vitro and in vivo, Biochem. J. 401 (2007) 29–38.

[10] A. Sitte, H. Paul, G. Hilgetag, Reaction of 2,5-diamino-1,3,4-thiadiazole with α-halo ketones, Z. Chem. 7 (1967) 341–342.

[11] N.P. Buu-Hoi, N.D. Xuong, T. Thu-Cuc, La Réaction des ω-Bromoacétophénones avec l'Amino-2 thiazole et les Amino-2 benzothiazoles, Bull. Soc. Chim. Fr. (1966) 1277–1279.

[12] A. Andreani, M. Granaiola, A. Leoni, A. Locatelli, R. Morigi, M. Rambaldi, M. Recanatini, G. Lenaz, R. Fato, C. Bergamini, Effects of new ubiquinone-imidazo[2,1-*b*]thiazoles on mitochondrial complex I (NADH-ubiquinone reductase) and on mitochondrial permeability transition pore, Bioorg. Med. Chem. 12 (2004) 5525–5532.

[13] A. Andreani, M. Rambaldi, A. Locatelli, Herbicidal activity of 5-haloimidazo [2,1-*b*]thiazoles, Collect. Czech. Chem. Comm. 56 (1991) 2436–2447.

[14] A. Andreani, A. Leoni, A. Locatelli, R. Morigi, M. Rambaldi, M. Recanatini, V. Garaliene, Potential antitumor agents. 29. Synthesis and potential coanthracyclinic activity of imidazo[2,1-*b*]thiazole guanylhydrazones, Bioorg. Med. Chem. 8 (2000) 2359–2366.

[15] A. Andreani, M. Granaiola, A. Leoni, A. Locatelli, R. Morigi, M. Rambaldi, G. Giorgi, V. Garaliene, Potential antitumor agents. 34. Synthesis and antitumor activity of guanylhydrazones from imidazo[2,1-*b*]thiazoles and from diimidazo[1,2-*a*:1,2-*c*]pyrimidine, Anticancer Res. 24 (2004) 203–212.

[16] T.L. Nguyen, R. Gussio, J.A. Smith, D.A. Lannigan, S.M. Hecht, D.A. Scudiero, R.H. Shoemaker, D.W. Zaharevitz, Homology model of RSK2 N-terminal kinase domain, structure-based identification of novel RSK2 inhibitors, and preliminary common pharmacophore, Bioorg. Med. Chem. 14 (2006) 6097–6105.

[17] A. Andreani, S. Burnelli, M. Granaiola, A. Leoni, A. Locatelli, R. Morigi, M. Rambaldi, L. Varoli, G. Farruggia, C. Stefanelli, L. Masotti, M.W. Kunkel, Synthesis and antitumor activity of guanylhydrazones from 6-(2,4-dichloro-5-nitrophenyl)- and 6-pyridyl-imidazo[2,1-*b*]thiazoles, J. Med. Chem. 49 (2006) 7897–7901.

[18] A. Andreani, M. Rambaldi, A. Leoni, A. Locatelli, R. Bossa, A. Fraccari, I. Galatulas, G. Salvatore, Potential antitumor agents. 24. Synthesis and pharmacological behavior of imidazo[2,1-*b*]thiazole guanylhydrazones bearing at least one chlorine, J. Med. Chem. 39 (1996) 2852–2855.

[19] J.A. Smith, D.J. Maloney, S.M. Hecht, D.A. Lannigan, structural basis for the activity of the RSK-specific inhibitor, SL0101, Bioorg. Med. Chem. 15 (2007) 5018–5034.

[20] I.A. Leighton, K.N. Dalby, F.B. Caudwell, P.T. Cohen, P. Cohen, Comparison of the specificities of p70 s6 kinase and MAPKAP kinase-1 identifies a relatively specific substrate for p70 s6 kinase: the N-terminal kinase domain of MAPKAP kinase-1 is essential for peptide phosphorylation, FEBS Lett. 375 (1995) 289–293.

[21] T.S.K. Eisinger-Mathasona, J. Andrade, D.A. Lannigan, RSK in tumorigenesis: connections to steroid signalling, Steroids 75 (2010) 191–202.

[22] A.G. Jobson, G.T. Lountos, P.L. Lorenzi, J. Llamas, J. Connelly, D. Cerna, J.E. Tropea, A. Onda, G. Zoppoli, S. Kondapaka, G. Zhang, N.J. Caplen, J.H. Cardellina II, S.S. Yoo, A. Monks, C. Self, D.S. Waugh, R.H. Shoemaker, Y. Yves Pommier, Cellular inhibition of checkpoint kinase 2 (Chk2) and potentiation of camptothecins and radiation by the novel Chk2 inhibitor PV1019 [7-Nitro-1H-indole-2-carboxylic acid {4-[1-(guanidinohydrazone)-ethyl]-phenyl}-amide], J. Pharmacol. Exp. Ther. 331 (2009) 816–826.

[23] A. Monks, D. Scudiero, P. Skehan, R. Shoemaker, K. Paull, D. Vistica, C. Hose, J. Langley, P. Cronise, A. Vaigro-Wolff, M. Gray-Goodrich, H. Campbell, J. Mayo, M. Boyd, Feasibility of a high-flux anticancer drug screen using a diverse panel of cultured human tumor cell lines, J. Natl. Cancer Inst. 83 (1991) 757–766.